

SHALLOW FOUNDATIONS RESTING ON STRONG SAND OVERLAYING WEAK SAND

A. HANNA¹, C. ABOU FARAH² AND M. ABDEL-RAHMAN³

ABSTRACT

Ultimate bearing capacity of shallow foundations under axial vertical loads resting on strong cohesionless soil overlying weak deposit was investigated. Previous studies addressed simplified failure mechanisms and punching shear failure mechanism. In this paper, stress analysis using the limit equilibrium method was performed on an assumed failure plane, which is believed to be close to the observed failure plane from experimental investigation available in the literature. Furthermore, the footing will fail by punching of the upper layer through to the lower by a truncated column making an angle α with the vertical. The results showed that the ultimate bearing capacity of a footing on a strong sand layer overlying weak sand deposit depends on the relative shear strength of the two layers, footing geometry, embedment depth, and the thickness of the upper sand layer. The theoretical model developed was validated with the available experimental data in the literature, where good agreement was noted.

KEYWORDS: Bearing capacity, Shallow foundations, Strong sand layer, Weak sand deposit, Limit equilibrium method of analysis.

1. INTRODUCTION

Foundation design necessitates that the ultimate bearing capacity of the soil is sufficient to support the proposed building, and that the settlement is within a tolerable limit. In the literature, the majority of the bearing capacity theories were developed for homogeneous soils, however, the ground is usually made of layered soils. Layered soil

¹ Professor, Department of Building, Civil and Environmental Engineering, Concordia University, Montreal, Quebec, Canada.

² Research Associate, Department of Building, Civil and Environmental Engineering, Concordia University, Montreal, Quebec, Canada.

³ Professor, Housing and Building National Research Center (HBRC), Giza, Egypt, mrahman.hbrc@gmail.com

profiles can be encountered in natural deposits or artificially made by adding a subgrade layer.

Brown and Meyerhof were first to investigate footing on a stiff clay layer overlying a soft clay layer. They assumed that the footing fails by punching through the top layer [1].

Meyerhof conducted an experimental investigation on the strip and circular footings on sand overlying clay: dense sand overlying soft clay and loose sand overlying stiff clay. The theories developed were validated with the experimental results obtained [2].

Meyerhof and Hanna conducted experimental and analytical investigations on footings on a strong layer overlying weak deposit and a weak layer overlying strong deposit. The theories developed compared well with the experimental data. The theories predict bearing capacity of these footings under vertical and inclined load [3].

Hanna and Meyerhof extended their theory of the ultimate bearing capacity of two-layer soils to the case of three-layer soils [4]. Pfeifle and Das conducted an experimental investigation. The results compared well with the predicted values of Meyerhof [2, 5].

Hanna extended the theory to cover the case of footings resting on subsoil consisting of a strong sand layer overlying weak sand deposit [6].

Madhav and Sharma developed a formula for the ultimate bearing capacity of footings resting on a sand layer over a soft clay layer using the punching shear mechanism developed by Meyerhof and Hanna [3, 7].

Radoslaw Et Al. used the kinematics approach of limit analysis to calculate average limit pressure under footings to predict the bearing capacity of footings resting on two-layer soil [8].

Kumar and Chakraborty investigated the bearing capacity of a circular footing on sand layer overlying cohesive deposit using the axisymmetric lower bound limit analysis together with finite elements and linear optimization. They reported that a certain optimum thickness of the sand layer exists beyond which no further improvement occurs [9].

Mosallanezhad and Moayedi conducted a comparative analysis of methods developed to predict bearing capacity of footing on layered soils, to include; experimental investigations, analytical models using limit equilibrium, and numerical models using finite element analyses. It was concluded that there are a number of factors influencing the bearing capacity of the soil, such as soil layer thickness, soil properties, applied stress, and the method of analysis [10].

Tang and Phoon compiled 159 centrifuge test results for footing on sand overlying clay deposit where punch-through the upper layer was observed [11].

Eshkevari Et Al. investigated the case of strip footings resting on a relatively thin layer of dense sand overlying a weaker sand layer. Finite Element Analysis was employed to calculate failure load and to identify the geometry of the failure mechanism [12]. In another study, an estimation of the undrained bearing capacity of a rigid strip footing on sand layer of finite thickness overlying clay deposit, using finite element limit analysis was carried out. The rigorous upper and lower bound theorems of plasticity were employed to bracket the bearing capacity of the footing, and to identify the geometry of failure mechanisms [13].

2. ANALYTICAL MODEL

The case of a shallow footings on a strong sand layer overlying a weak sand deposit subjected to vertical load was considered. It was reported that the footing is punching in a roughly truncated parabolic shape into the lower sand layer [14]. In this analysis, the failure mechanism was idealized as a truncated column punching through the upper layer to the lower layer using the limit equilibrium method of analysis. Figure 1 presents the considered strip footing having a width, B and depth D , resting on dense sand layer overlying loose sand deposit. The thickness of the upper sand layer is H below the footing base. The unit weight and angle of shearing resistance of the upper and lower sand layers are γ_1 , ϕ_1 and γ_2 , ϕ_2 , respectively.

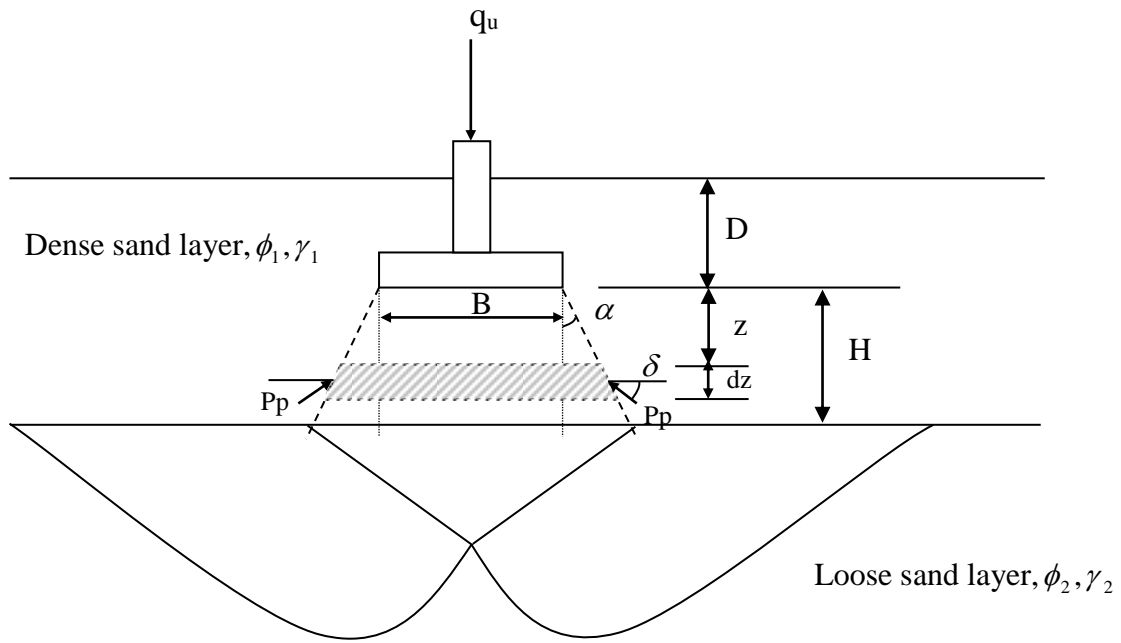


Fig. 1. Punching shear mechanism of a strip footing on dense sand overlying loose sand deposit.

Figure 2 presents a horizontal strip at a depth z from the founding level having a thickness dz . The strip is subjected to a passive earth pressure P_p , acting on the failure plane at an average angle δ upwards, and vertical stress (σ_{zz}) acting on the top of the strip, the vertical stress ($\sigma_{zz} + d\sigma_{zz}$) acting upward on the bottom of the strip, and the weight of the slice, W .

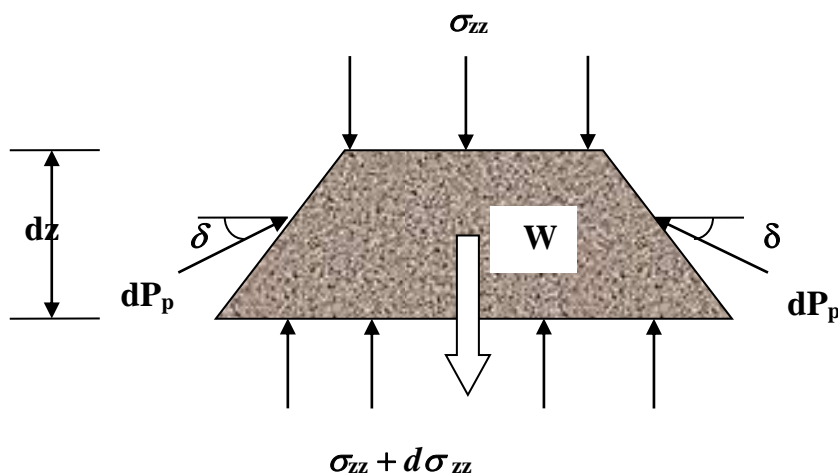


Fig. 2. Forces acting on a strip dz of the failure zone at depth z .

Where:

- σ_{zz} : Vertical stress acting on the top of the slice.
 $\sigma_{zz} + d\sigma_{zz}$: Vertical stress acting upward on the bottom of slice.
 B : Width of the footing.
 D : Embedment depth of the footing.
 Z : Depth of the slice from the founding level.
 α : Angle of the assumed failure plane with the vertical.
 δ : Mobilized angle of shearing resistance on the assumed failure plane.
 γ_1 : Unit weight of the upper sand layer.
 K_p : Coefficient of passive earth pressure given by Caquot and Kerisel [15].
 dP_p : Passive earth pressure, acting on the sides of the punching slice:

$$dP_p = \gamma_1 \left(D + z + \frac{dz}{2} \right) K_p \quad (1)$$

Employing the limit equilibrium technique of the vertical forces, Eq. (2) equation is obtained as

$$\begin{aligned} \sigma_{zz}(B + 2z \tan \alpha) - (\sigma_{zz} + d\sigma_{zz}) * [B + 2(z + dz) \tan \alpha] - 2 dP_{pv} dz \\ + \gamma_1 \left(B + 2\left(z + \frac{dz}{2}\right) \tan \alpha \right) dz = 0 \end{aligned} \quad (2)$$

Simplification of Eq. (2), gives Eq. (3) in the form

$$\begin{aligned} -\sigma_{zz}(2dz \tan \alpha) - d\sigma_{zz} * [B + 2(z + dz) \tan \alpha] - 2dP_{pv} dz + \gamma_1 \left(B + \right. \\ \left. 2\left(z + \frac{dz}{2}\right) \tan \alpha \right) dz = 0 \end{aligned} \quad (3)$$

The value of $\sigma_{zz}(2dz \tan \alpha)$ is too small and can be reasonably assumed to be equal to zero. Thus Eq. (3) can be written as

$$-d\sigma_{zz}[B + 2(z + dz) \tan \alpha] - 2dP_{pv} dz + \gamma_1 \left(B + 2\left(z + \frac{dz}{2}\right) \tan \alpha \right) dz = 0 \quad (4)$$

$$\begin{aligned} d\sigma_{zz}[B + 2(z + dz) \tan \alpha] \\ = -2 \left[\gamma_1 k_p \left(D + z + \frac{dz}{2} \right) \right] \sin \delta dz + \gamma_1 [B + 2 \left(z + \frac{dz}{2} \right) \tan \alpha] dz \end{aligned} \quad (5)$$

Multiplying and rearranging the factors in Eq. (5), the following can be produced:

$$d\sigma_{zz}(B + 2(z + dz)\tan \alpha) = -2\gamma_1 K_p D \sin \delta dz - 2\gamma_1 K_p z \sin \delta dz - \gamma_1 K_p \sin \delta dz dz + \gamma_1 \left(B + 2 \left(z + \frac{dz}{2} \right) \tan \alpha \right) dz \quad (6)$$

The following components of Eq. (6) are too small and can be neglected:

$$\gamma_1 K_p \sin \delta dz dz, \gamma_1 \frac{dz}{2} \tan \alpha, \text{ and } 2dz \tan \alpha = 0 \quad (7)$$

Thus Eq. (6) can be written as

$$d\sigma_{zz} = -\frac{2\gamma_1 K_p D \sin \delta}{B + 2z \tan \alpha} dz + \frac{-2\gamma_1 K_p \sin \delta}{B + 2z \tan \alpha} z dz + \gamma_1 dz \quad (8)$$

Integrating Eq. (8) gives

$$\int d\sigma_{zz} = \int -\frac{2\gamma_1 K_p D \sin \delta}{B + 2z \tan \alpha} dz + \int \frac{-2\gamma_1 K_p \sin \delta}{B + 2z \tan \alpha} z dz + \int \gamma_1 dz \quad (9)$$

$$\text{Let } A_1 = -2\gamma_1 K_p D \sin \delta \quad (10)$$

$$\text{and } A_2 = -2\gamma_1 K_p \sin \delta \quad (11)$$

$$\sigma_{zz} = \int \frac{A_1 dz}{B + 2z \tan \alpha} + \int \frac{A_2 z dz}{B + 2z \tan \alpha} + \int \gamma_1 dz \quad (12)$$

$$(I) \quad (II) \quad (III)$$

The stress σ_{zz} is the sum of the three integrals I, II, and III, which can be solved separately as follows:

$$\text{Integral (I):} \quad A_1 \int \frac{dz}{B + 2z \tan \alpha} \quad (13)$$

In order to solve this integral let $u = B + 2z \tan \alpha$, then $du = 2 \tan \alpha * dz$, and $dz = \frac{du}{2 \tan \alpha}$

Substitute the value of dz , and then integral (I) can be written as

$$A_1 \int \frac{du}{2 \tan \alpha} \frac{1}{u} = \frac{A_1}{2 \tan \alpha} \ln u + c = \frac{A_1}{2 \tan \alpha} (\ln(B + 2z \tan \alpha)) + c \quad (14)$$

$$\begin{aligned} \text{Integral (II):} \quad & \int \frac{A_2 z dz}{B + 2z \tan \alpha} \\ &= \frac{A_2}{(2 \tan \alpha)^2} [B + 2z \tan \alpha - B(\ln(B + 2z \tan \alpha))] + c \end{aligned} \quad (15)$$

$$\text{Integral (III):} \quad \int \gamma_1 dz = \gamma_1 z + c \quad (16)$$

Where: c is a constant.

Substituting Eqs. (14-16) in Eq. (12), the following equation can be written:

$$\sigma_{zz} = \frac{-\gamma_1 K_p D \sin \delta}{\tan \alpha} \ln(B + 2z \tan \alpha) + \frac{-2 \gamma_1 K_p \sin \delta}{(2 \tan \alpha)^2} [B + 2z \tan \alpha - B \ln(B + 2z \tan \alpha)] + \gamma_1 + c \quad (17)$$

In order to determine the value of the constant c , the following boundary conditions were considered: z varies from 0 to H , where H is the depth of the upper layer below the footing base. At $z = 0$ (the slice is just below the footing) the stress $\sigma_{zz} = q_u$, and Eq. (17) can be written as

$$q_u = \frac{A_1}{2 \tan \alpha} \ln(B) + \frac{A_2}{(2 \tan \alpha)^2} (B - B \ln(B)) + c \quad (18)$$

Where: q_u is the ultimate bearing capacity of the footing on two-layered soil.

Replacing A_1 and A_2 by their values;

$$q_u = \frac{-\gamma_1 K_p D \sin \delta}{\tan \alpha} \ln(B) - \frac{\gamma_1 K_p \sin \delta}{(2 \tan \alpha)^2} * B(1 - \ln B) + c \quad (19)$$

The value of the constant c can be calculated as

$$c = q_u + \frac{\gamma_1 K_p \sin \delta}{\tan \alpha} * [D \ln B + \frac{B(1 - \ln B)}{2 \tan \alpha}] \quad (20)$$

Refer to Fig. (2), at $z = H$; (interface slice), the stress $\sigma_{zz} = q_b$

Where: q_b is the ultimate bearing capacity of the footing on a thick bed of the lower layer; q_b can be evaluated as

$$q_b = \frac{1}{2} \gamma_2 B N_{\gamma_2} + \gamma_1 (H + D) N_{q_2} \quad (\text{for sand layer}) \quad (21)$$

$$q_b = C_u N_{c_2} + \gamma_1 (H + D) \quad (\text{for clay layer}) \quad (22)$$

Where:

N_{γ_2} , N_{q_2} , and N_{c_2} are the bearing capacity factors for strip footings resting on a thick bed of the lower layer (weak sand deposit).

Replacing z with H and σ_{zz} with q_b , the following equation can be obtained.

$$\sigma_{zz} = \frac{A_1}{2 \tan \alpha} \ln(B + 2H \tan \alpha) + \frac{A_2}{(2 \tan \alpha)^2} [B + 2H \tan \alpha - B \ln(B + 2H \tan \alpha)] + \gamma_1 H + c \quad (23)$$

Substituting the values of A_1 , A_2 and c in Eq. (23) gives

$$q_b = \frac{-2\gamma_1 K_p D \sin\delta}{2 \tan \alpha} \ln(B + 2H \tan \alpha) + \frac{-2 \gamma_1 K_p \sin \delta}{(2 \tan \alpha)^2} [B + 2H \tan \alpha - B \ln(B + 2H \tan \alpha)] + \gamma_1 H + q_u + \frac{\gamma_1 K_p \sin \delta}{\tan \alpha} [D \ln B + \frac{B (1 - \ln B)}{2 \tan \alpha}] \quad (24)$$

Rearranging and simplifying Eq. (24) gives

$$q_u = q_b - \gamma_1 H + \frac{\gamma_1 K_p D \sin\delta}{\tan \alpha} [\ln(B + 2H \tan \alpha) - \ln B] + \frac{\gamma_1 K_p \sin \delta}{(2 \tan \alpha)^2} [B + 2H \tan \alpha - B \ln(B + 2H \tan \alpha) - B + B \ln B] \quad (25)$$

$$\text{Assuming that } F = \ln(B + 2H \tan \alpha) - \ln B = \ln\left[\frac{B + 2H \tan \alpha}{B}\right] \quad (26)$$

After simplification, Eq. (25) can be written as

$$q_u = q_b - \gamma_1 H + \frac{\gamma_1 K_p \sin\delta}{\tan \alpha} [DF + \frac{2H \tan \alpha - BF}{2 \tan \alpha}] \quad (27)$$

Or in a dimensionless form by dividing both sides by $\gamma_1 B$ as

$$\frac{q_u}{\gamma_1 B} = \frac{q_b}{\gamma_1 B} + \frac{K_p \sin\delta}{\tan \alpha} \left[\frac{DF}{B} + \frac{H}{B} - \frac{F}{2 \tan \alpha} \right] - \frac{H}{B} \quad (28)$$

The parameters used in Eq. (28) were described above. K_p is the coefficient of passive earth pressure for the upper sand layer, is taken from Caquot and Kerisel [15], which depends on the angle of shearing resistance ϕ_1 and the ratio δ/ϕ_1 , where the angle δ is the mobilized angle of shearing resistance on the assumed failure planes. The following arguments are considered:

- 1- If the analysis were made on actual failure planes, the angle δ will be equal to ϕ_1 , if however, the analysis is made on assumed failure planes, the angle δ , mobilized on the assumed failure planes is used, which is less than ϕ_1 , as failure has not yet taken place on this plane.
- 2- The assumed failure planes are considered the best-fit straight line to the actual failure planes.
- 3- The angle δ varies with the depth of the upper layer, which decreases as the assumed failure planes deviate from the actual failure plane (curved). Thus the angle δ will be equal to ϕ_1 when both the assumed and the actual failure planes coincide with each other.

In this analysis, the ratio (δ/ϕ_1) will be assumed as 0.9. This is justified as the assumed failure plane is the best-fit line to the actual curved one.

The non-dimensional ratio $\frac{q_b}{\gamma_1 B}$ can be written as

$$\frac{q_b}{\gamma_1 B} = \frac{1}{2} \frac{\gamma_2}{\gamma_1} N_{\gamma 2} + \frac{H + D}{B} N_{q 2} \quad (29)$$

In order to determine the angle α , the experimental data reported by Hanna given in Table 1 were employed [6]. The deduced angles α are given in Table 2 and presented in Fig. 3.

Accordingly, the values of the angle α shown in Fig. 3 are only valid within the range of $H/B = 0.5$ to 4.5 , then the predicted values will be in agreement with the experimental results presented in this paper and the data available in the literature.

The ratio q_2/q_1 varies between 0 and 1, since the case of a strong upper layer overlying a weak deposit is considered in this study. A value of q_2/q_1 equal to 1 refers to the homogenous case, where according to Terzaghi [16], the failure below the footing occurs with an angle α equal to $(45 + \phi_1/2)$ with the vertical.

For the given experimental data shown in Table 1:

$$\frac{q_2}{q_1} = \frac{\gamma_2}{\gamma_1} \frac{N_{\gamma 2}}{N_{\gamma 1}} = \frac{13.8 * 41.06}{16.3 * 468.3} = 0.074 \quad (30)$$

Where:

q_2 : ultimate bearing capacity of footing resting on a very thick bed of layer 2.

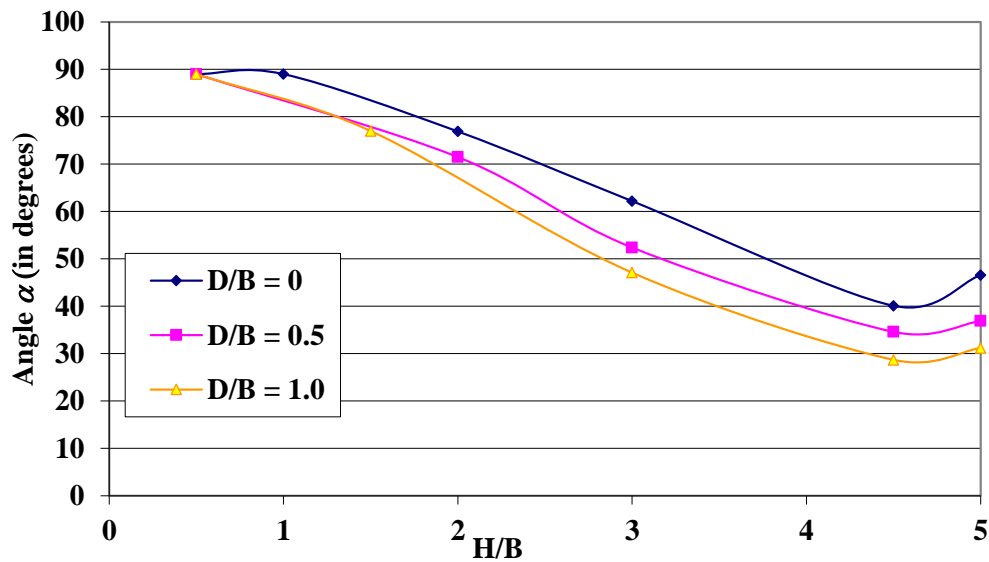
q_1 : ultimate bearing capacity of footing resting on a very thick bed of layer 1.

Table 1. Soil properties used in experimental investigation [6].

Top Layer (Strong Sand)	Bottom Layer (Weak Sand)
$\phi_1 = 47.7$ degrees	$\phi_2 = 34.0$ degrees
$\gamma_1 = 16.3$ kN/m ³	$\gamma_2 = 13.8$ kN/m ³
$N_{\gamma 1} = 468.3$	$N_{\gamma 2} = 41.06$
$N_{q 1} = 211.8$	$N_{q 2} = 29.44$

Table 2. Deduced angle α from the experimental results reported [6].

Experimental Data			Calculated Angle α
D/B	H/B	q_u (kN/m ²)	(degrees)
0.0	1.0	36.68	89.0
	2.0	72.74	76.9
	3.0	120.94	62.2
	4.5	231.74	40.1
	5.0	237.88	46.6
0.50	0.5	36.27	89.0
	2.0	101.43	71.5
	3.0	170.03	52.4
	4.5	303.45	34.6
	5.0	323.86	36.9
1.0	0.5	48.40	89.0
	1.5	99.84	77.0
	3.0	219.61	47.1
	4.5	391.77	28.7
	5.0	412.46	31.2

Fig. 3. Deduced angle α vs. H/B for different D/B ratios, from the experimental results of Hanna [6].

3. Considerations for the Angle α

The first step towards predicting the behavior of the angle α is to determine the parameters on which it depends, which are as follows:

- 1- The ratio H/B (depth of the upper sand layer over the footing's width).
- 2- The ratio q_2/q_1 (ultimate bearing capacity of the lower layer over the ultimate bearing capacity of the upper layer taken as homogenous)
- 3- The angle of shearing resistance of the upper sand layer ϕ_1 .
- 4- The ratio δ/ϕ_1 (the mobilized angle of shearing resistance on the assumed failure planes δ over the angle of shearing resistance of the upper sand layer ϕ_1).
- 5- The ratio D/B (depth of the footing in the upper sand layer over the footing's width).

Three trials were reported by Abou Farah to predict the angle α by assuming a certain function for the angle α while the rest of the parameters were varied in order to calculate the ratio δ/ϕ_1 , which varies between 0 and 1 [14].

Also, the ratio q_2/q_1 varies between 0 and 1 for the case of strong upper layer overlying weak deposit. A value of q_2/q_1 equals to 1 refers to the homogenous case, where according to Terzaghi, the failure occurs with an angle α equal to $(45 + \phi_1/2)$ with the vertical [16].

A value of q_2/q_1 equal to 0 refers to either case scenario, q_2 tends to zero or q_1 tends to ∞ . In the first scenario, if the upper layer is overlying a fluid, the punching occurs rapidly and vertically, and the corresponding angle α equals to zero. In the second scenario, if the footing is lying on a very strong upper layer, like rock or concrete, there will be no punching, and at ultimate load failure occurs horizontally in the upper strong layer, and the angle α tends to 90° .

The first trial assumed that the angle α is a function of the ratio q_2/q_1 with a parabolic equation. By using the available experimental data and back calculating the ratio δ/ϕ_1 . The deduced values of the ratio δ/ϕ_1 were not consistent with the condition that it lies between 0 and 1. Therefore, the assumed parabolic equation of the angle α is not valid.

The second trial assumed that the angle α is a straight line, assuming that the angle α is equal to 0 for $q_2/q_1 = 0$ and equal to $(45 + \phi_1/2)$ for $q_2/q_1 = 1$. Calculating the angle α using the available experimental data and by back calculating the ratio δ/ϕ_1 , the deduced values for the ratio δ/ϕ_1 were not consistent with the condition that it should be between 0 and 1, accordingly the assumed function is also not valid.

The third and the last trial takes into consideration all parameters involved and gives a series of equations to calculate the angle α . Assuming that the ratio δ/ϕ_1 is equal to 0.90 (constant), the equation for the angle α has the following form:

$$\alpha = \rho \ln (q_2/q_1) + \mu \quad (31)$$

Where:

- ρ : Function of the ratios H/B and D/B
 μ : Function of the angle of shearing resistance of the upper layer ϕ_1 ,
 $\mu = 45 + \phi_1/2$

The equation for ρ is a straight line with the ratio H/B and may be expressed as

$$\rho = \lambda (H/B) + \theta \quad (32)$$

Where the constants λ and θ are determined according to the back calculations, and their values are presented in Table 3.

Table 3. Values for the constants λ and θ

D/B	λ	θ
0	4.108	-9.159
0.50	4.577	-9.420
1.00	4.513	-9.960

Detailed calculations can be found in Abou Farah [14].

4. VALIDATION OF THE PROPOSED BEARING CAPACITY EQUATION

The theory developed in this paper was validated with the experimental results of Hanna [6]. It can be noted that a good agreement was obtained for lower values of H/B as the system acts as a two-layer system, while for higher values of H/B the system tends to function as footing on homogeneous upper layer sand. Figures 4-6

present the comparison between theoretical and experimental results for the cases $D/B=0$, 0.5, and 1.0 respectively.

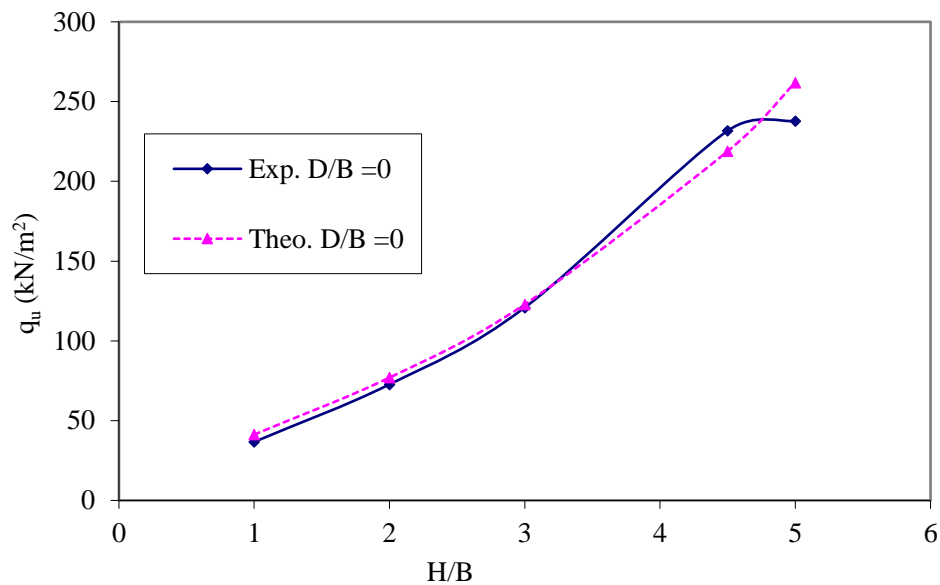


Fig. 4. Comparison of theoretical values of q_u at $D/B=0$ with experimental results of Hanna [6].

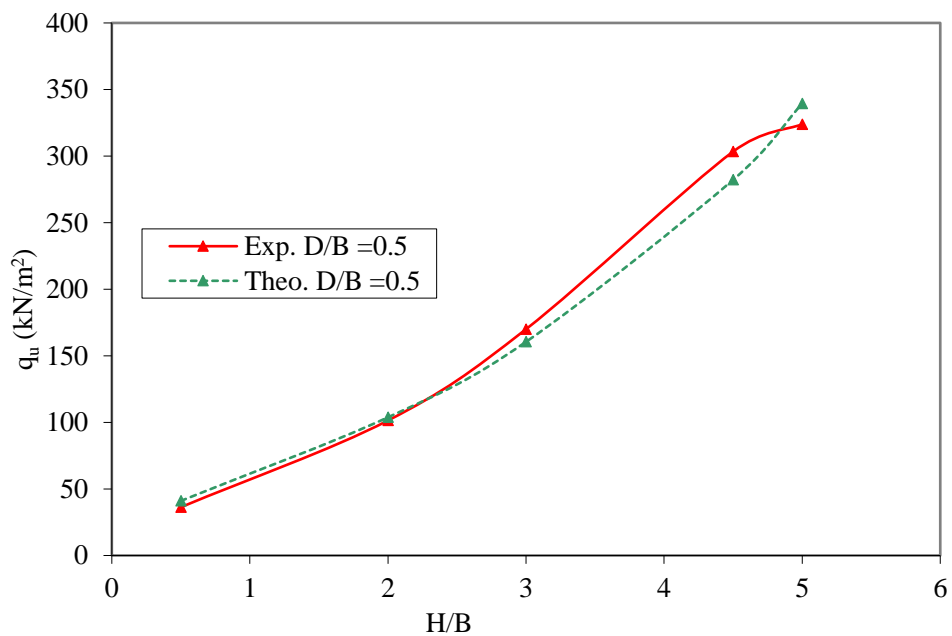


Fig. 5. Comparison of theoretical values of q_u at $D/B=0.50$ with experimental results of Hanna [6].

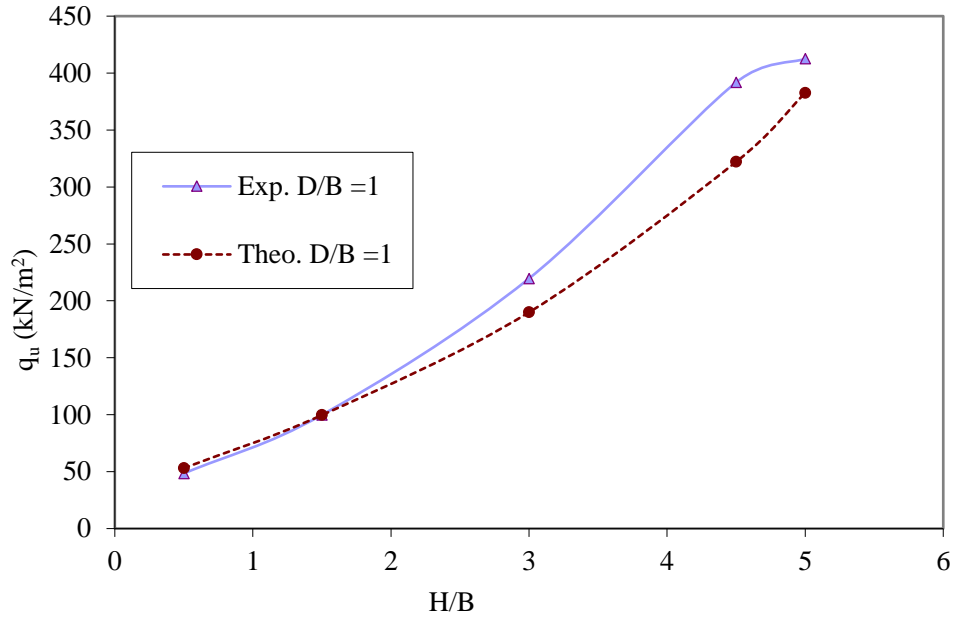


Fig. 6. Comparison of theoretical values of q_u at $D/B=1$ with experimental results of Hanna [6].

5. CONCLUSIONS

The case of footing on strong sand layer overlying a weak sand deposit was investigated. The following conclusions are obtained:

1. Stress analysis was performed on an assumed failure mechanism. In this analysis, the mobilization shear strength on the failure planes was considered.
2. A design formula was developed to predict the bearing capacity as a function of the shear strength of the upper and lower layers, the footing depth/width ratio and the measured angle of the failure plane with respect to the vertical.
3. The predicted values of the bearing capacity using the proposed formula compared well with the experimental data presented by Hanna [6].
4. The comparison between theoretical and experimental values of the bearing capacity were varied between 1% and 13% for lower values of H/B , and it reaches 17% for values of the ratio H/B of 4.5 and 5, where the homogeneous case prevails as presented in Figs 4-6.

ACKNOWLEDGMENTS

This research was supported financially by the National Research Council of Canada (NRC).

DECLARATION OF CONFLICT OF INTERESTS

The authors have declared no conflict of interests.

REFERENCES

1. Brown, J. D., and Meyerhof, G. G., "Experimental Study of Bearing Capacity in Layered Clays", Proceedings of the 7th International Conference on Soil Mechanics and Foundation Engineering, Mexico, Vol. 2, pp. 45-51, 1969.
2. Meyerhof, G. G., "Ultimate Bearing Capacity of Footings on Sand Layer Overlying Clay", Canadian Geotechnical Journal, Vol. 11, pp. 223-229, 1974.
3. Meyerhof, G. G., and Hanna, A. M., "Ultimate Bearing Capacity of Foundations on Layered Soils under Inclined Load", Canadian Geotechnical Journal, Vol. 15, No. 4, pp. 565-572, 1978.
4. Hanna, A. M., and Meyerhof G. G., "Ultimate Bearing Capacity of Foundations on a Three-Layer Soil", with Special Reference to Layered Sand, Canadian Geotechnical Journal, Vol. 16, No. 2, pp. 412-414, 1979.
5. Pfeifle, T. W., and Das, B. M., "Model Tests for Bearing Capacity in Sand", Journal of Geotechnical Engineering, ASCE, 105(GT9), pp. 1112-1116, 1979.
6. Hanna, A. M., "Foundations on Strong Sand Overlying Weak Sand", Journal of Geotechnical Engineering, 107(GT7), pp. 915-927, 1981.
7. Madhav, M. R., and Sharma, J. S. N., "Bearing Capacity of Clay Overlain by Stiff Soil", Journal of Geotechnical Engineering, Vol. 117, No. 12, pp. 1941-1947, 1991.
8. Michalowski, R. L. and Shi, L., "Bearing Capacity of Footings over Two-Layer Foundation Soils", Journal of Geotechnical Engineering, Vol. 121, No. 5, pp. 421-428, 1995.
9. Kumar, G. and Chakraborty, M., "Bearing Capacity of a Circular Foundation on layered Sand-Clay Media", The Japanese Geotechnical Society, Soils and Foundations, Vol. 55, No. 5, pp. 1058-1068, 2015.
10. Mosallanezhad, M., and Moayedi, H., "Comparison Analysis of Bearing Capacity Approaches for the Strip Footing on Layered Soils", Arabian Journal for Science and Engineering, Vol. 42, pp. 3711-3722, 2017.
11. Tang, C., and Phoon, K.K., "Evaluation of Stress-Dependent Methods for the Punch-Through Capacity of Foundations in Clay with Sand", ASCE-ASME Journal of Risk and Uncertainty in Engineering Systems, Part A: Civil Engineering, Vol. 5, No. 3, Article 04019008, pp. 1-18, 2019.
12. Eshkevari, S.S., Abbo, A. J., and Kouretzis, G., "Bearing Capacity of Strip Footings on Layered Sands", Computer and Geotechnics, Vol. 114, Article 103101, pp. 1-11, 2019.

13. Eshkevari, S. S., Abbo, A. J., and Kouretzis, G., "Bearing Capacity of Strip Footings on Sand Over Clay", Canadian Geotechnical Journal, Vol. 56, pp. 699-709, 2019.
14. Abou Farah, C., "Ultimate Bearing Capacity of Shallow Foundations on Layered Soils", M.Sc. Thesis, Department of Building, Civil and Environmental Engineering, Concordia University, Montreal, Canada, 2004.
15. Caquot, A., and Kerisel, J., "Tables de Poussee et Butee", Gauthier-Villars, Paris, 1948.
16. Terzaghi, K., "Theoretical Soil Mechanics", Wiley, New York, p. 121, 1943.

الاساسات الضحلة المرتكزة على طبقة رمل قوية تعلو طبقة رمل ضعيفة

يدرس البحث قدرة التحمل القصوى للأساسات الضحلة المعرضة للأحمال الرأسية المحورية المرتكزة على تربة مكونة من طبقة رمل قوية تعلو طبقة رمل ضعيفة، وقد استخدمت الدراسات السابقة اليات مبسطة لشكل الانهيار والية انهيار القص الاختراقي اما في البحث الحالي تم تحليل الاجهادات بطريقة التوازن الحدي على منحنى الانهيار المفترض والذي يعتقد أنه قريب من منحنى الانهيار الملاحظ في الاختبارات المعملية بالإضافة أن الاساس سوف ينهار عن طريق اختراق طبقة التربة العلوية من خلال الطبقة السفلية على شكل عمود مقطوع يصنع زاوية (الفا) مع الرأسى، وتظهر النتائج أن قدرة التحمل القصوى للأساس المرتكز على طبقة رمل قوية تعلو طبقة رمل ضعيفة تعتمد على الاجهاد النسبي للطبقتين والخصائص الهندسية للاساس وعمق التأسيس وسمك طبقة الرمل العلوية، وبمقارنة نتائج النموذج النظري بنتائج اختبارات معملية منشورة سابقا تبين وجود تتطابق بينهما بصورة جيدة.